



**18th IAEA Fusion Energy Conference
Sorrento, Italy, 4 to 10 October 2000**

IAEA-CN-77/EXP4/18

NATIONAL INSTITUTE FOR FUSION SCIENCE

Impact of Pellet Injection on Extension of Operational Region in LHD

R. Sakamoto, H. Yamada, K. Tanaka, K. Narihara, S. Morita, S. Sakakibara, S. Masuzaki, L.R. Baylor, P.W. Fisher, S.K. Combs, M.J. Gouge, S. Kato, A. Komori, O. Kaneko, N. Ashikawa, P. de Varies, M. Emoto, H. Funaba, M. Goto, K. Ida, H. Idei, K. Ikeda, S. Inagaki, M. Isobe, S. Kado, K. Kawahata, K. Khlopenkov, S. Kubo, R. Kumazawa, T. Minami, J. Miyazawa, T. Morisaki, S. Murakami, S. Muto, T. Mutoh, Y. Nagayama, Y. Nakamura, H. Nakanishi, K. Nishimura, N. Noda, T. Notake, T. Kobuchi, Y. Liang, S. Ohdachi, N. Ohyabu, Y. Oka, M. Osakabe, T. Ozaki, R.O. Pavlichenko, B.J. Peterson, A. Sagara, K. Saito, H. Sasao, M. Sasao, K. Sato, M. Sato, T. Seki, T. Shimozuma, M. Shoji, S. Sudo, H. Suzuki, M. Takechi, Y. Takeiri, N. Tamura, K. Toi, T. Tokuzawa, Y. Torii, K. Tsumori, I. Yamada, S. Yamaguchi, S. Yamamoto, Y. Yoshimura, K.Y. Watanabe, T. Watari, K. Yamazaki, Y. Hamada, O. Motojima and M. Fujiwara

(Received - Sep. 12, 2000)

NIFS-648

Sep. 2000

This report was prepared as a preprint of work performed as a collaboration research of the National Institute for Fusion Science (NIFS) of Japan. This document is intended for information only and for future publication in a journal after some rearrangements of its contents.

Inquiries about copyright and reproduction should be addressed to the Research Information Center, National Institute for Fusion Science, Oroshi-cho, Toki-shi, Gifu-ken 509-02 Japan.

RESEARCH REPORT NIFS Series

This is a preprint of a paper intended for presentation at a scientific meeting. Because of the provisional nature of its content and since changes of substance or detail may have to be made before publication, the preprint is made available on the understanding that it will not be cited in the literature or in any way be reproduced in its present form. The views expressed and the statements made remain the responsibility of the named author(s); the views do not necessarily reflect those of the government of the designating Member State(s) or of the designating organization(s). In particular, neither the IAEA nor any other organization or body sponsoring this meeting can be held responsible for any material reproduced in this preprint.

TOKI, JAPAN

Impact of Pellet Injection on Extension of Operational Region in LHD

R. Sakamoto¹⁾, H. Yamada¹⁾, K. Tanaka¹⁾, K. Narihara¹⁾, S. Morita¹⁾, S. Sakakibara¹⁾, S. Masuzaki¹⁾, L.R. Baylor²⁾, P.W. Fisher²⁾, S.K. Combs²⁾, M.J. Gouge²⁾, S. Kato¹⁾, A. Komori¹⁾, O. Kaneko¹⁾, N. Ashikawa³⁾, P. de Varies¹⁾, M. Emoto¹⁾, H. Funaba¹⁾, M. Goto¹⁾, K. Ida¹⁾, H. Idei¹⁾, K. Ikeda¹⁾, S. Inagaki¹⁾, M. Isobe¹⁾, S. Kado¹⁾, K. Kawahata¹⁾, K. Khlopenkov¹⁾, S. Kubo¹⁾, R. Kumazawa¹⁾, T. Minami¹⁾, J. Miyazawa¹⁾, T. Morisaki¹⁾, S. Murakami¹⁾, S. Muto¹⁾, T. Mutoh¹⁾, Y. Nagayama¹⁾, Y. Nakamura¹⁾, H. Nakanishi¹⁾, K. Nishimura¹⁾, N. Noda¹⁾, T. Notake⁴⁾, T. Kobuchi³⁾, Y. Liang³⁾, S. Ohdachi¹⁾, N. Ohyabu¹⁾, Y. Oka¹⁾, M. Osakabe¹⁾, T. Ozaki¹⁾, R.O. Pavlichenko¹⁾, B.J. Peterson¹⁾, A. Sagara¹⁾, K. Saito⁴⁾, H. Sasao³⁾, M. Sasao¹⁾, K. Sato¹⁾, M. Sato¹⁾, T. Seki¹⁾, T. Shimozuma¹⁾, M. Shoji¹⁾, S. Sudo¹⁾, H. Suzuki¹⁾, M. Takechi¹⁾, Y. Takeiri¹⁾, N. Tamura³⁾, K. Toi¹⁾, T. Tokuzawa¹⁾, Y. Torii⁴⁾, K. Tsumori¹⁾, I. Yamada¹⁾, S. Yamaguchi¹⁾, S. Yamamoto⁴⁾, Y. Yoshimura¹⁾, K.Y. Watanabe¹⁾, T. Watari¹⁾, K. Yamazaki¹⁾, Y. Hamada¹⁾, O. Motojima¹⁾ and M. Fujiwara¹⁾

1) National Institute for Fusion Science, Toki, Japan

2) Oak Ridge National Laboratory, Oak Ridge, TN, USA

3) Department of Fusion Science, Graduate University for Advanced Studies, Hayama, Japan

4) Department of Energy Engineering and Science, Nagoya University, Nagoya, Japan

E-mail. sakamoto@LHD.nifs.ac.jp

Abstract: Pellet injection has been used as a primary fueling scheme in Large Helical Device (LHD). Pellet injection has extended an operational region of NBI plasmas to higher densities with maintaining preferable dependence of energy confinement on density, and achieved several important data, such as plasma stored energy (0.88 MJ), energy confinement time (0.3 s), β (2.4 % at 1.3 T) and density ($1.1 \times 10^{20} \text{ m}^{-3}$). These parameters cannot be attained by gas puffing.

Ablation and subsequent behavior of plasma has been investigated. Measured pellet penetration depth that is estimated by duration of the $H\alpha$ emission is shallower than predicted penetration depth from the simple neutral gas shielding (NGS) model. The penetration depth can be explained by NGS model with fast ion effect on the ablation. Just after ablation, redistribution of ablated pellet mass was observed in short time ($\sim 400 \mu\text{s}$). The redistribution causes shallow deposition and low fueling efficiency.

1. Introduction

Through the study of inter-machine scalings of energy confinement time [1,2], confinement in currentless helical plasmas has been proved to be comparable to in tokamaks while preferable dependence on electron density is more pronounced than in tokamaks. The international stellarator scaling 95 (ISS95) is described as follows.

$$\tau_E^{\text{ISS95}} = 0.079 a_p^{2.21} R_0^{0.65} P_{\text{abs}}^{-0.59} \bar{n}_e^{0.51} B_0^{0.83} \tau_{2/3}^{0.40}.$$

Gas puffing has been successful for building up and sustaining the plasma density in the past generation fusion plasma experiments. However, inevitability of gas puffing is questionable in large-scale, high-temperature and steady state fusion plasmas since the plasma sources are strongly localized at the plasma surface. Especially gas puffing is not efficient in LHD, because the core plasma region is surrounded with the thick ergodic layer that connects to the divertor. Efficient fueling to the core plasma would be mandatory in large plasmas. Hydrogen ice pellet injection is one of the important techniques used for core plasma fueling. In the LHD experiment, pellet injector is placed as a fundamental tool since deterioration of fueling efficiency by gas puffing is a concern.

The ablation mechanism and the subsequent density redistribution affect fueling efficiency and fueling depth [3,4]. Since a dramatic increase in pellet velocity, which can enhance deep fueling, poses a difficult problem in technology, optimization based on physical understanding of the mechanism of these processes is required.

The main aim of the present study is to reveal pellet ablation behavior and effect of pellet injection on plasma, and to examine the validity of the pellet fueling in LHD.

2. Experimental set-up

Experiments were carried out on Large Helical Device (LHD), a heliotron type magnetic confinement device with super conducting coils [5,6]. The major radius, averaged minor radius, magnetic field and plasma volume are 3.9 m, 0.6 m, 2.9 T and 30 m^3 , respectively.

The pellet injector used on LHD is a pneumatic pipe-gun type accelerator with a GM cycle refrigerator [7]. The injector is equipped with five barrels and can inject independently any desired time. The mass and velocity of pellets are $0.4 - 1.0 \times 10^{21}$ atoms per pellet and 900 - 1200 m/s, respectively. Cylindrical pellets formed from high purity hydrogen gas were injected horizontally from the outer side mid-plane of LHD. Pellet mass was measured by a microwave cavity mass detector, and velocity was measured by the time of flight method. The injected pellets were checked by a shadow graph system, which consists of a fast flash lamp and a CCD camera at the exit of the injector.

Pellet injection experiment has been carried out mainly for NBI heated plasmas. LHD is equipped with two negative-ion based neutral beam injectors. The range of beam energy and port through power is 120 - 150 keV and 1 - 4.5 MW, respectively.

Pellet ablation was measured by a fast photo diode (500 kHz sampling) and a CCD camera (each 33 ms exposure) with a $\text{H}\alpha$ (656.5 nm) filter. A variety diagnostics were used to investigate the plasma behavior after pellet injection. For instance, line-averaged electron densities \bar{n}_e were measured by a 13-chord vertical view far-infrared (FIR) laser interferometer [8], which was installed at the distance 168° in the toroidal angle from the pellet injection port. Profiles of electron temperature T_e and electron density n_e were measured by the multi-point (200) Thomson scattering system [9], which was installed at the distance 30° in toroidal angle. Electron density profile based on Thomson scattering was calibrated by Abel inverted FIR interferometer data just before pellet injection.

3. Extension of operational region following pellet injections

Waveforms for typical pellet injected discharge are shown in figure 1. Pellet injection was carried out at 0.8, 0.88, 0.96, 1.04 and 1.12 s. The line averaged electron

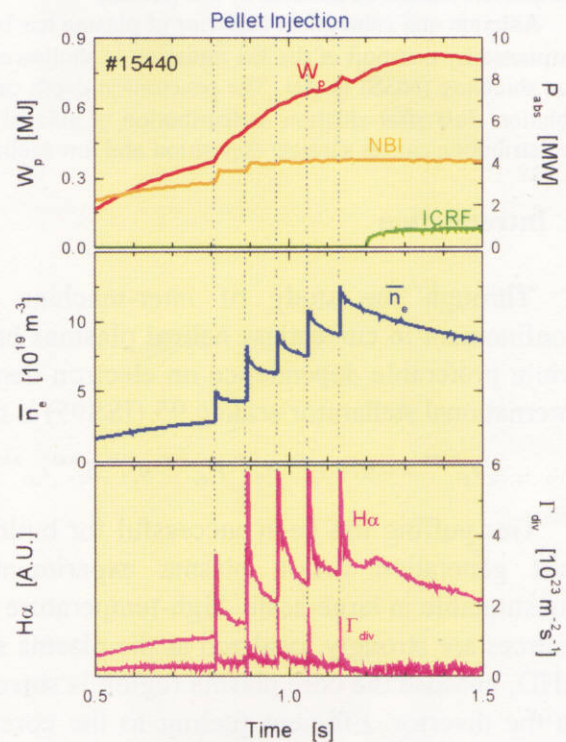


Figure 1. Waveform of typical pellet injected discharge. (#15440, $B_t = 2.75 \text{ T}$, $R_{ax} = 3.6 \text{ m}$, $P_{NBI} = 4 \text{ MW}$).

density increases sharply at each pellet injection and a burst in the H α intensity and divertor flux is observed simultaneously. Figure 2 shows plots of the normalized maximum stored energy versus the density when the stored energy achieved to maximum. Predicted dependence by the international stellarator scaling 95 (ISS95) is shown with dashed lines. Since systematic enhancement in energy-confinement time from the scaling has been observed in LHD [10], 1.7 times of the prediction is also shown. In the case of gas puffing, confinement degradation was observed at density above $0.35 \times 10^{20} \text{ m}^{-3}$ and the maximum density is $0.5 \times 10^{20} \text{ m}^{-3}$. On the other hand, in the pellet injection discharges no obvious density-related confinement degradation has been observed beyond predicted the density limit, and the stored energy reaches to 0.88 MJ.

Figure 3 shows maximum line averaged electron density versus NBI power. Solid line indicate the predicted density limit in the stellarator/heliotron device. The density limit can be expressed as follows [2],

$$n_c^s = 0.25 \sqrt{PB/a^2 R}.$$

where P , B , a and R are the heating power, the magnetic field strength, the minor radius and the major radius, respectively. In the case of gas puffing, an envelope of the data conforms well to the predicted density limit. In the case of pellet injection, the maximum density reaches to high density beyond predicted density limit.

4. Ablation behaviors and density redistribution

Neutral gas shielding (NGS) model [11][12], which is the most widely adopted ablation model. If one assumes pellet injection normal to the plasma from the outside midplane and linear profiles for electron temperature and density, the penetration depth scaling of the NGS models is expressed as follows [13],

$$\lambda/a = C T_e^{-5/9} n_e^{-1/9} m_p^{5/27} v_p^{1/3},$$

where T_e , n_e , m_p and V_p are the central electron temperature, the central electron density, the pellet mass and the pellet velocity, respectively. The scaling suggests that the penetration depth

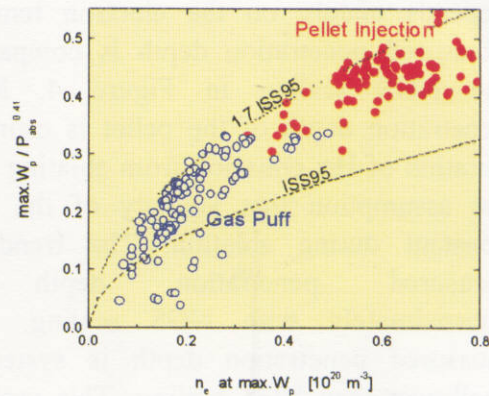


Figure 2. Normalized maximum plasma stored energy versus line averaged electron density. Open circle and close circle indicate data of gas puffing and pellet injection, respectively. Dashed line show ISS95 scaling prediction.

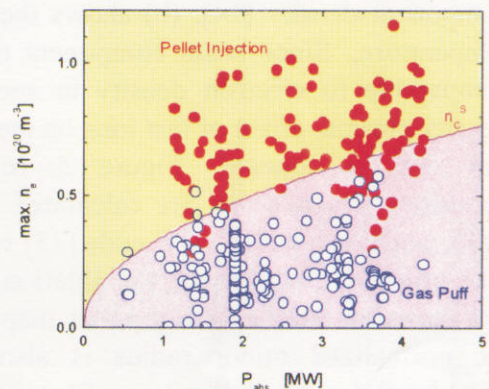


Figure 3. Maximum line averaged electron density versus NBI power. Open circle and close circle indicate data of gas puffing and pellet injection, respectively. predicted density limit is show with solid line.

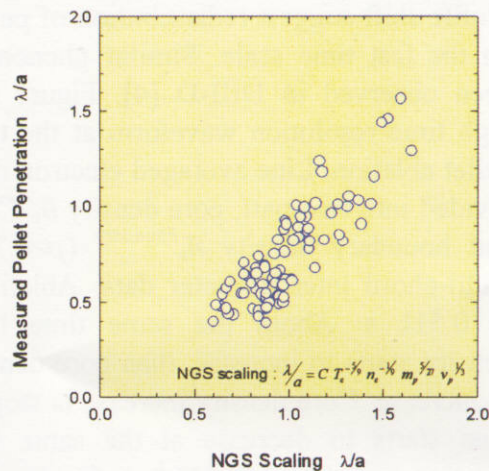


Figure 4. Comparison of the measured penetration depth versus the scaling.

depends mainly on the electron temperature. Measured penetration depth is compared with the NGS scaling in Figure 4. Measured penetration depth of the pellet is estimated by duration of H α emission from ablating pellet on the assumption that velocity of the pellet is constant during ablation. The trend of the measured penetration depth agrees approximately with NGS scaling, but the measured penetration depth is systematically shallower than NGS scaling. This systematic difference can be explained by effect of fast ions on the ablation. There is no Ohmic heating in LHD and the NBI is only heating source. Figure 5 shows the profiles before and after pellet injection into 3.1 MW NBI heated plasma. (a) shows the density and calculated beam component density [14]. (b) shows the electron temperature. Since beam component density is comparable to electron density in such a low density plasma, effect of fast ions on the ablation can not be ignored. Figure 5 (c) shows deposition profiles that are calculated from the NGS model using ABLATE code [15] which can take effect of fast ions on the ablation, and the H α emission from ablating pellet mapped onto the normalized minor radius is also shown. Calculated deposited density profile with fast ion ablation indicates a good agreement with H α emission measurement. On the other hand, measured deposition peak is shifted outward as compared with H α emission peak, and majority of pellet mass was deposited outside of $\rho = 0.8$. As a result, a net fueling efficiency is 46 %. This profile shift suggest redistribution of pellet mass on the fast time scale. Similar phenomena has been observed in DIII-D [4]. Figure 6 shows high time resolution waveform at the timing of pellet ablation. Line averaged electron density is divided into two part, core density \bar{n}_e^{core} ($\rho < 0.7$) and boundary density $\bar{n}_e^{boundary}$ ($\rho > 0.7$), using multi-chord interferometer data. Ablation starts at 0.511 s. About the same time boundary density starts to increase, then core density start to increase. Core density increase is stopped and then starts to decrease at the same time the ablation is finished (0.5114 s). Contrary to this, boundary density increases further. The core

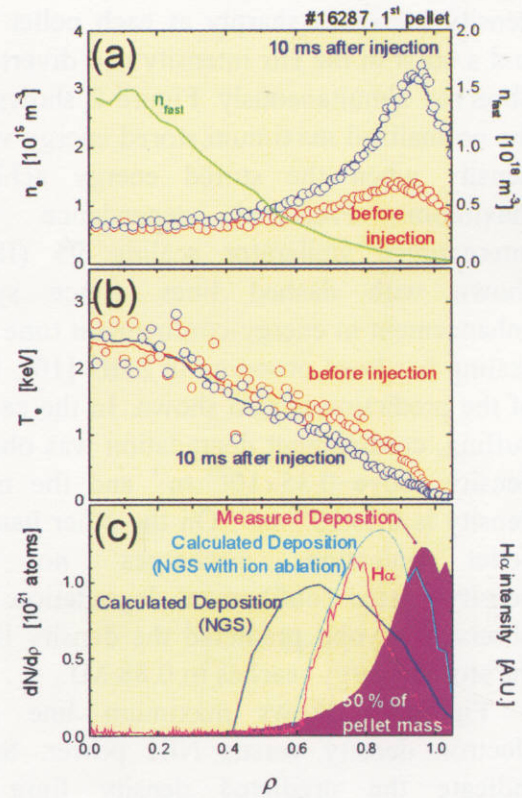


Figure 5. Radial profiles before and after pellet injection. (a) electron density and calculated beam component density, (b) electron temperature, (c) H α intensity which indicates pellet penetration depth, measured deposition and calculated deposition.

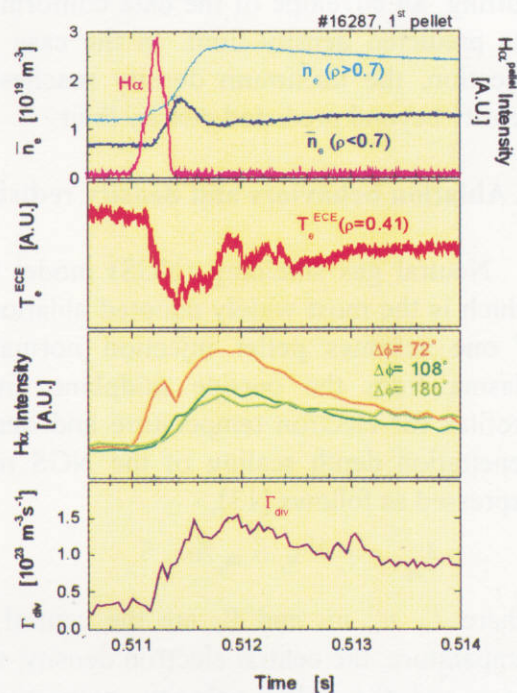


Figure 6. Temporal evolution of pellet injected plasma at the timing of ablation.

density decrease and boundary density increase stop at 0.5118 s (400 μ s after ablation). These phenomena can be explained as follows. Though pellet penetrates into a certain depth that is well predicted by the NGS with fast ion ablation, a noticeable part of pellet mass are spewed out from the core region, pellet mass redistribute in a short time (\sim 400 μ s). On the other hand, electron temperature at $\rho=0.41$ indicate the inverse behavior to core density evolution, therefore pellet mass redistribute adiabatically. H α emission except for ablating pellet grows in the core density decay phase which is distinct in the apart toroidal position, and divertor flux also increase at the same time.

5. Summary and future plan

Pellet injection has extended an operational region of NBI plasmas to higher densities with maintaining preferable dependence of the energy confinement on the density beyond the gas-fueling conditions. At the current stage of experiment, attained density was restricted by the supply mass of the pellet and/or the lack of heating power. A hard density limit has not been observed in LHD yet, it is an important issue to investigate on the confinement property and density limit in the further high density regime in helical systems.

Though penetration depth of the pellet is explained qualitatively by a simple NGS model, when fast ion effect on the ablation is considered in NGS model, a quantitative agreement between measurement and calculation has been obtained. However, expulsion of the pellet mass was observed on the fast time scale (\sim several 100 μ s) just after ablation, which causes degradation of fueling efficiency. Because a same phenomenon is observed in tokamak, it is considered that there is a general physical mechanism on density redistribution. Improvement of the pellet fueling by means of the magnetic high field side injection has been reported in tokamak [3][4]. We have plan of inner port injection in the coming LHD experimental campaign which start at the beginning of October, 2000. The mechanism on density redistribution will be revealed through comparative study in different magnetic configurations.

The authors are grateful to the device-engineering group for their operational support.

Reference

- [1] Stroth, U., et al., Nuclear Fusion, 36 (1996) 1063-1077
- [2] Sudo, s., et al., Nuclear Fusion, 30 (1990) 11-21.
- [3] Lang, P.T., et al., Physical Review Letters, 79 (1997) 1487-1490
- [4] Baylor, L.R., et al., Fusion Technology, 34 (1998) 425-429
- [5] Fujiwara, M., et al., Journal of Fusion Energy, 15 (1996) 7-153
- [6] Motojima, O., et al., Physics of Plasmas, 6 (1999) 1843-1850.
- [7] Yamada, H., et al., to be published on Fusion Engineering and Design
- [8] Kawahata, K., et al., Fusion Engineering and Design, 34-35 (1997) 393-397.
- [9] Narihara, K., et al., Fusion Engineering and Design, 34-35 (1997) 67-72.
- [10] Yamada, H., et al., Physical Review Letter, 84 (2000) 1216-1219.
- [11] Parks, P.B., et al., Nuclear Fusion, 17 (1977) 539-556.
- [12] Milora, S L., et al., IEEE Transaction on Plasma Science, PS-6 (1978) 578-592.
- [13] Baylor, L.R., et al., Nuclear Fusion, 37 (1997) 445-450
- [14] Murakami, S., et al., Fusion Technology, 27 (1995) 256-259
- [15] Nakamura, N., et al., Nuclear Fusion, 26 (1986) 907-921

Recent Issues of NIFS Series

- NIFS-588 W.X. Wnag, N. Nakajima, S. Murakami and M. Okamoto,
An Accurate δf Method for Neoclassical Transport Calculation, Mar. 1999
- NIFS-589 K. Kishida, K. Araki, S. Kishiba and K. Suzuki,
Local or Nonlocal? Orthonormal Divergence-free Wavelet Analysis of Nonlinear Interactions in Turbulence; Mar. 1999
- NIFS-590 K. Araki, K. Suzuki, K. Kishida and S. Kishiba,
Multiresolution Approximation of the Vector Fields on T^3 , Mar. 1999
- NIFS-591 K. Yamazaki, H. Yamada, K.Y. Watanabe, K. Nishimura, S. Yamaguchi, H. Nakanishi, A. Komori, H. Suzuki, T. Mito, H. Chikaraishi, K. Murai, O. Motojima and the LHD Group,
Overview of the Large Helical Device (LHD) Control System and Its First Operation, Apr. 1999
- NIFS-592 T. Takahashi and Y. Nakao,
Thermonuclear Reactivity of D-T Fusion Plasma with Spin-Polarized Fuel, Apr. 1999
- NIFS-593 H. Sugama,
Damping of Toroidal Ion Temperature Gradient Modes; Apr. 1999
- NIFS-594 Xiaodong Li,
Analysis of Crowbar Action of High Voltage DC Power Supply in the LHD ICRF System, Apr. 1999
- NIFS-595 K. Nishimura, R. Horiuchi and T. Sato,
Drift-kink Instability Induced by Beam Ions in Field-reversed Configurations, Apr. 1999
- NIFS-596 Y. Suzuki, T.-H. Watanabe, T. Sato and T. Hayashi,
Three-dimensional Simulation Study of Compact Toroid Plasmoid Injection into Magnetized Plasmas; Apr. 1999
- NIFS-597 H. Sanuki, K. Itoh, M. Yokoyama, A. Fujisawa, K. Ida, S. Toda, S.-I. Itoh, M. Yagi and A. Fukuyama,
Possibility of Internal Transport Barrier Formation and Electric Field Bifurcation in LHD Plasma; May 1999
- NIFS-598 S. Nakazawa, N. Nakajima, M. Okamoto and N. Ohyaibu,
One Dimensional Simulation on Stability of Detached Plasma in a Tokamak Divertor, June 1999
- NIFS-599 S. Murakami, N. Nakajima, M. Okamoto and J. Nhrenberg,
Effect of Energetic Ion Loss on ICRF Heating Efficiency and Energy Confinement Time in Heliotrons, June 1999
- NIFS-600 R. Horiuchi and T. Sato,
Three-Dimensional Particle Simulation of Plasma Instabilities and Collisionless Reconnection in a Current Sheet, June 1999
- NIFS-601 W. Wang, M. Okamoto, N. Nakajima and S. Murakami,
Collisional Transport in a Plasma with Steep Gradients; June 1999
- NIFS-602 T. Mutoh, R. Kumazawa, T. Saki, K. Saito, F. Simpo, G. Nomura, T. Watari, X. Jikang, G. Cattanei, H. Okada, K. Ohkubo, M. Sato, S. Kubo, T. Shimozuma, H. Idei, Y. Yoshimura, O. Kaneko, Y. Takeiri, M. Osakabe, Y. Oka, K. Tsumon, A. Komori, H. Yamada, K. Watanabe, S. Sakakibara, M. Shoji, R. Sakamoto, S. Inagaki, J. Miyazawa, S. Morita, K. Tanaka, B.J. Peterson, S. Murakami, T. Minami, S. Ohdachi, S. Kado, K. Narihara, H. Sasao, H. Suzuki, K. Kawahata, N. Ohyaibu, Y. Nakamura, H. Funaba, S. Masuzaki, S. Muto, K. Sato, T. Morigaki, S. Sudo, Y. Nagayama, T. Watanabe, M. Sasao, K. Ida, N. Noda, K. Yamazaki, K. Akaishi, A. Sagara, K. Nishimura, T. Ozaki, K. Toi, O. Motojima, M. Fujiwara, A. Iyoshi and LHD Exp Group 1 and 2,

- First ICRF Heating Experiment in the Large Helical Device; July 1999
- NIFS-603 P.C de Vries, Y Nagayama, K Kawahata, S Inagaki, H. Sasao and K Nagasaki,
Polarization of Electron Cyclotron Emission Spectra in LHD; July 1999
- NIFS-604 W. Wang, N. Nakajima, M. Okamoto and S. Murakami,
 δf Simulation of Ion Neoclassical Transport; July 1999
- NIFS-605 T. Hayashi, N. Mizuguchi, T. Sato and the Complexity Simulation Group,
Numerical Simulation of Internal Reconnection Event in Spherical Tokamak; July 1999
- NIFS-606 M. Okamoto, N. Nakajima and W. Wang,
On the Two Weighting Scheme for δf Collisional Transport Simulation; Aug. 1999
- NIFS-607 O. Motojima, A.A. Shishkin, S. Inagaki, K.Y. Watanabe,
Possible Control Scenario of Radial Electric Field by Loss-Cone-Particle Injection into Helical Device; Aug. 1999
- NIFS-608 R. Tanaka, T. Nakamura and T. Yabe,
Constructing Exactly Conservative Scheme in Non-conservative Form; Aug. 1999
- NIFS-609 H. Sugama,
Gyrokinetic Field Theory, Aug 1999
- NIFS-610 M. Takechi, G. Matsunaga, S. Takagi, K. Ohkuni, K. Toi, M. Osakabe, M. Isobe, S. Okamura, K. Matsuoka, A. Fujisawa, H. Iguchi, S. Lee, T. Minami, K. Tanaka, Y. Yoshimura and CHS Group,
Core Localized Toroidal Alfvén Eigenmodes Destabilized By Energetic Ions in the CHS Heliotron/Torsatron, Sep. 1999
- NIFS-611 K. Ichiguchi,
MHD Equilibrium and Stability in Heliotron Plasmas; Sep. 1999
- NIFS-612 Y. Sato, M. Yokoyama, M. Wakatani and V. D. Puzovtsov,
Complete Suppression of Pfirsch-Schluter Current in a Toroidal $I=3$ Stellarator; Oct. 1999
- NIFS-613 S. Wang, H. Sanuki and H. Sugama,
Reduced Drift Kinetic Equation for Neoclassical Transport of Helical Plasmas in Ultra-low Collisionality Regime; Oct. 1999
- NIFS-614 J. Miyazawa, H. Yamada, K. Yasui, S. Kato, N., Fukumoto, M. Nagata and T. Uyama,
Design of Spheromak Injector Using Conical Accelerator for Large Helical Device; Nov. 1999
- NIFS-615 M. Uchida, A. Fukuyama, K. Itoh, S.-I. Itoh and M. Yagi,
Analysis of Current Diffusive Ballooning Mode in Tokamaks; Dec. 1999
- NIFS-616 V. Tanaka, A. Yu. Grosberg and T. Tanaka,
Condensation and Swelling Behavior of Randomly Charged Multichain Polymers by Molecular Dynamics Simulations; Dec 1999
- NIFS-617 S. Goto and S. Kida,
Sparseness of Nonlinear Coupling; Dec. 1999
- NIFS-618 M.M. Skoric, T. Sato, A. Maluckov and M.S. Jovanovic,
Complexity in Laser Plasma Instabilities Dec. 1999
- NIFS-619 T.-H. Watanabe, H. Sugama and T. Sato,
Non-dissipative Kinetic Simulation and Analytical Solution of Three-mode Equations of Ion Temperature Gradient Instability; Dec. 1999

- NIFS-620 Y Oka, Y. Takeiri, Yu I. Belchenko, M. Hamabe, O. Kaneko, K. Tsumori, M. Osakabe, E. Asano, T. Kawamoto, R. Akiyama,
Optimization of Cs Deposition in the 1/3 Scale Hydrogen Negative Ion Source for LHD-NBI System, Dec 1999
- NIFS-621 Yu I. Belchenko, Y. Oka, O. Kaneko, Y. Takeiri, A. Krivenko, M. Osakabe, K. Tsumori, E. Asano, T. Kawamoto, R. Akiyama,
Recovery of Cesium in the Hydrogen Negative Ion Sources, Dec 1999
- NIFS-622 Y. Oka, O. Kaneko, K. Tsumori, Y. Takeiri, M. Osakabe, T. Kawamoto, E. Asano, and R. Akiyama,
H⁻ Ion Source Using a Localized Virtual Magnetic Filter in the Plasma Electrode Type I LV Magnetic Filter: Dec 1999
- NIFS-623 M. Tanaka, S. Kida, S. Yanase and G. Kawahara,
Zero-absolute-vorticity State in a Rotating Turbulent Shear Flow, Jan. 2000
- NIFS-624 F. Leuterer, S. Kubo,
Electron Cyclotron Current Drive at $\omega \approx \omega_c$ with X-mode Launched from the Low Field Side; Feb. 2000
- NIFS-625 K. Nishimura,
Wakefield of a Charged Particulate Influenced by Emission Process of Secondary Electrons; Mar. 2000
- NIFS-626 K. Itoh, M. Yagi, S.-I. Itoh, A. Fukuyama,
On Turbulent Transport in Burning Plasmas, Mar. 2000
- NIFS-627 K. Itoh, S.-I. Itoh, L. Giannone,
Modelling of Density Limit Phenomena in Toroidal Helical Plasmas; Mar. 2000
- NIFS-628 K. Akaishi, M. Nakasuga and Y. Funato,
True and Measured Outgassing Rates of a Vacuum Chamber with a Reversibly Absorbed Phase; Mar. 2000
- NIFS-629 T. Yamagishi,
Effect of Weak Dissipation on a Drift Orbit Mapping; Mar. 2000
- NIFS-630 S. Toda, S.-I. Itoh, M. Yagi, A. Fukuyama and K. Itoh,
Spatial Structure of Compound Dither in L/H Transition; Mar. 2000
- NIFS-631 N. Ishihara and S. Kida,
Axial and Equatorial Magnetic Dipoles Generated in a Rotating Spherical Shell; Mar. 2000
- NIFS-632 T. Kuroda, H. Sugama, R. Kanno and M. Okamoto,
Ion Temperature Gradient Modes in Toroidal Helical Systems, Apr. 2000
- NIFS-633 V.D. Pustovitov,
Magnetic Diagnostics: General Principles and the Problem of Reconstruction of Plasma Current and Pressure Profiles in Toroidal Systems, Apr. 2000
- NIFS-634 A.B. Mikhailovskii, S.V. Konovalov, V.D. Pustovitov and V.S. Tsypin,
Mechanism of Viscosity Effect on Magnetic Island Rotation, Apr. 2000
- NIFS-635 H. Naitou, T. Kuramoto, T. Kobayashi, M. Yagi, S. Tokuda and T. Matsumoto,
Stabilization of Kinetic Internal Kink Mode by Ion Diamagnetic Effects; Apr. 2000
- NIFS-636 A. Kageyama and S. Kida,
A Spectral Method in Spherical Coordinates with Coordinate Singularity at the Origin, Apr. 2000

- NIFS-637 R. Horuchi, W. Pei and T. Sato,
Collisionless Driven Reconnection in an Open System: June 2000
- NIFS-638 K. Nagaoka, A. Okamoto, S. Yoshimura and M.Y. Tanaka,
Plasma Flow Measurement Using Directional Langmuir Probe under Weakly Ion-Magnetized Conditions; July 2000
- NIFS-639 Alexei Ivanov,
Scaling of the Distribution Function and the Critical Exponents near the Point of a Marginal Stability under the Vlasov-Poisson Equations; Aug. 2000
- NIFS-640 K. Ohr, H. Naitou, Y. Tauchi, O. Fukumasa,
Observation of the Limit Cycle in the Asymmetric Plasma Divided by the Magnetic Filter; Aug. 2000
- NIFS-641 H. Momota, G.H. Miley and J. Nadler,
Direct Energy Conversion for IEC Propulsions; Aug. 2000
- NIFS-642 Y. Kondoh, T. Takahashi and H. Momota,
Revisit to the Helicity and the Generalized Self-organization Theory; Sep. 2000
- NIFS-643 H. Soltwisch, K. Tanaka,
Changes of the Electron Density Distribution during MHD Activity in CHS: Sep 2000
- NIFS-644 Fujisawa, A., Iguchi, H., Minami, T., Yoshimura, Y., Sanuki, H., Itoh, K., Isobe, M., Nishimura, S., Tanaka, K., Osakabe, M., Nomura, I., Ida, K., Okamura, S., Toi, K., Kado, S., Akiyama, R., Shimizu, A., Takahashi, C., Kojima, M., Matsuoka, K., Hamada, Y., Fujiwara, M.,
Observation of Bifurcation Property of Radial Electric Field Using a Heavy Ion Beam Probe: Sep. 2000
(IAEA-CN-77/EX6/6)
- NIFS-645 Todo, Y., Watanabe, T.-H., Park, H.-B., Sato, T.,
Fokker-Planck Simulation Study of Alfvén Eigenmode Burst Sep. 2000
(IAEA-CN-77/TH6/2)
- NIFS-646 Muroga, T., Nagasaka, T.,
Development of Manufacturing Technology for High Purity Low Activation Vanadium Alloys: Sep. 2000
(IAEA-CN-77/FTP1/09)
- NIFS-647 Itoh, K., Sanuki, H., Toda, S., Itoh, S.-I., Yagi, M., Fukuyama, A., Yokoyama, M.,
Theory of Dynamics in Long Pulse Helical Plasmas: Sep. 2000
(IAEA-CN-77/THP1/19)
- NIFS-648 R. Sakamoto, H. Yamada, K. Tanaka, K. Narihara, S. Morita, S. Sakakibara, S. Masuzaki, L.R. Baylor, P.W. Fisher, S.K. Combs, M.J. Gouge, S. Kato, A. Komori, O. Kaneko, N. Ashikawa, P. de Varies, M. Emoto, H. Funaba, M. Goto, K. Ida, H. Idei, K. Ikeda, S. Inagaki, M. Isobe, S. Kado, K. Kawahata, K. Khlopenkov, S. Kubo, R. Kumazawa, T. Minami, J. Miyazawa, T. Morisaki, S. Murakami, S. Muto, T. Mutoh, Y. Nagayama, Y. Nakamura, H. Nakanishi, K. Nishimura, N. Noda, T. Notake, T. Kobuchi, Y. Liang, S. Ohdachi, N. Ohyaabu, Y. Oka, M. Osakabe, T. Ozaki, R.O. Pavlichenko, B.J. Peterson, A. Sagara, K. Saito, H. Sasao, M. Sasao, K. Sato, M. Sato, T. Seki, T. Shimozuma, M. Shoji, S. Sudo, H. Suzuki, M. Takechi, Y. Takeiri, N. Tamura, K. Toi, T. Tokuzawa, Y. Torii, K. Tsumori, I. Yamada, S. Yamaguchi, S. Yamamoto, Y. Yoshimura, K.Y. Watanabe, T. Watari, K. Yamazaki, Y. Hamada, O. Motojima and M. Fujiwara,
Impact of Pellet Injection on Extension of Operational Region in LHD: Sep. 2000
(IAEA-CN-77/EXP4/18)/